







Photostabilization Mechanisms of Polyvinyl Chloride Using Schiff Base Compounds

Mahmood Mohammed Ahmed¹, Mohammed Alwan Farhan², Maha Salih Hussein¹,
Ekhlas Abdallah Hassan^{2*}

¹ Department of Chemistry, College of Education, University of Samarra, Samarra 34010, Iraq

² Department of Chemistry, College of Sciences, University of Diyala, Diyala 32001, Iraq

Corresponding Author Email: ekhlasbiochemistry@gmail.com

Copyright: ©2026 The authors. This article is published by IETA and is licensed under the CC BY 4.0 license (<http://creativecommons.org/licenses/by/4.0/>).

<https://doi.org/10.18280/ijdne.210413>

ABSTRACT

Received: 14 February 2026

Revised: 7 April 2026

Accepted: 18 April 2026

Available online: 30 April 2026

Keywords:

Schiff base, polyvinyl chloride, photostabilizer, ultraviolet irradiation, Field Emission Scanning Electron Microscopy, electrical conductivity, quantum yield of chain scission, intersystem crossing

Three Schiff base compounds were synthesized, characterized, and evaluated as photostabilizing additives for polyvinyl chloride (PVC) tends to experience breakdown of its polymer chains when subjected to ultraviolet (UV) light or elevated temperatures, leading to a reduction in its mechanical strength, chemical stability, and overall performance. This limits its practical use, especially in outdoor environments. To enhance PVC's resistance to such photodegradation, the Schiff base compounds M4, M9, and MM4 were incorporated into the polymer chain at a concentration of 0.9 %wt. and cast into films with a thickness of 40 μm . These films were then exposed to UV irradiation at a wavelength of 365 nm to evaluate the effectiveness of the additives in protecting the polymer chains from UV-induced damage. The accelerated weathering test was carried out using ultraviolet light with an intensity 2.2×10^{-6} Einstein $\cdot \text{dm}^{-3} \cdot \text{s}^{-1}$, which corresponds approximately to 18 Watts per square meter (W/m^2) at room temperature for a total exposure period of 300 hours. The extent of photodegradation was systematically evaluated using Fourier Transform Infrared (FTIR) spectroscopy, UV and visible light Spectroscopy, and electrical conductivity measurements obtained via an Inductance, Capacitance, and Resistance (LCR) meter. Key parameters, including the carbonyl index (CI), viscosity-average molecular weight (\overline{M}_v), and photodegradation rate constant (k_d), were determined. In addition, surface morphological changes of the irradiated polymer films were examined. The experimental results confirmed that the incorporation of Schiff base additives significantly improved the photostability of PVC. The CI values were calculated from the FTIR spectra, after 300 h of irradiation. The CI decreased from 0.602 to 0.2711, and the photodegradation rate constant (k_d) was significantly reduced from (9.02×10^{-3}) to (8.06×10^{-3}) in the presence of M4 compared to blank PVC. Among the investigated compounds, M4 exhibited the highest stabilization efficiency, effectively suppressing degradation processes. The enhanced performance of M4 was attributed to multiple photostabilization mechanisms, including UV absorption, radical scavenging, internal conversion (IC), and intersystem crossing (ISC). Consequently, compound M4 exhibited the highest photostabilization efficiency among the tested compounds.

1. INTRODUCTION

The majority of plastics manufactured are designed for short-term uses, whereas approximately one-fourth is allocated for long-term applications, like piping. This short-term usage has led to an annual rise in plastic waste, resulting in improper disposal in the environment [1]. Polyvinyl chloride (PVC) is among the earliest thermoplastic polymers. Since the onset of PVC manufacturing in the Early 1930s, its production volume has consistently increased. It is currently ranked as the third most produced polymer worldwide in terms of production size [2]. PVC is characterized by distinct mechanical and physical properties, with the chemical structure represented by the repeating unit $(\text{CH}_2-\text{CHCl})_n$. It is a colorless, inflexible polymer with quite high density and a low melting temperature, and it is mainly classified as a

thermoplastic material [3]. PVC is widely used because of several favorable characteristics, including low manufacturing cost, ease of processing into various shapes, resistance to acids and alkalis, and inherent flame-retardant behavior. Consequently, it has extensive applications in construction materials, flooring systems, cables, pipes, window frames, and many other products [4]. Despite these advantages, PVC exhibits limited resistance to environmental factors such as ultraviolet (UV) radiation and elevated temperatures. Exposure to these conditions can induce structural changes in the polymer chains, leading to deterioration in both physical and chemical properties through a phenomenon known as photodegradation [5]. During photodegradation, reactive species, including peroxides, hydrogen chloride, and free radicals, are generated, which accelerate the degradation process. This mechanism involves the cleavage of carbon-

carbon bonds, resulting in chain scission [6]. These degradation processes are accompanied by observable changes, including discoloration of PVC from white to yellow, surface cracking, and weight loss. Such effects arise from the elimination of segments from the polymer backbone and the volatilization of degraded fragments, ultimately reducing the material's structural integrity and performance [7]. The poor photostability of PVC therefore restricts its use in applications exposed directly to sunlight. To overcome this limitation, photostabilization treatments are required to slow down or inhibit the photodegradation process. The photostabilization plays a vital role in improving the durability and service life of polymeric materials in outdoor environments [8]. The addition of suitable stabilizing additives during PVC processing is an effective approach to extending the operational lifetime of the polymer [9]. Additive materials used with PVC necessarily possess several important characteristics [10]; they should be compatible with the polymer, non-volatile, cost-effective, stable, readily available, and active [11]. Additionally, these additives need to avoid the creation of hydrogen chloride and be compatible with PVC for the absorption of UV rays that lead to photodegradation. By converting these harmful UV rays into energy far from the surface of the PVC, the additives help maintain the original color of the polymer over time and avoid the creation of polyene groups within the polymeric concatenation [12]. It has been discovered that additives that hold nanomaterials (such as TiO₂) and minerals (like Zn) can act as plasticizers for the polymer and help absorption (HCl) [13]. However, some of these additives are toxic and pose risks to human health and the environment, which makes their use inadvisable [14]. Although presence of numerous stabilizing agents, conventional additives frequently exhibit major drawbacks, including environmental persistence, toxicity, compromised long-term durability, and the tendency to emigrate from the polymer chain [15]. Consequently, contemporary investigations are oriented toward developing stabilizers that optimize PVC performance without compromising ecological and human safety. Within this framework, heterocyclic and Schiff bases have appeared as effective photostabilizers for PVC, their efficacy stems from their ability to absorb UV light and dissipate the absorbed energy through non-destructive pathways [16]. This paradigm shift aligns with the plastics industry's accelerating transition toward sustainable stabilization methodologies [17]. So, the current study utilizes eco-friendly Schiff base derivatives to accomplish the photostabilization of PVC [18]. These synthesized compounds reinforce the matrix of polymer via pathways predominantly UV shielding and free radical scavenging thereby functioning as primary stabilizers [19]. This stabilization mechanism substantially represses PVC chain scission, ultimately enhancing material durability and decreasing its environmental footprint [20]. Consequently, the photoprotective efficiency of these compounds was systematically evaluated under UV irradiation. The efficiency of the proposed additives was assessed using Fourier Transform Infrared (FTIR), UV-Visible spectroscopy, and FESEM. Electrical conductivity was used to monitor PVC photodegradation, where its increase is linked to bond breakdown (C-Cl), free radicals and double bonds form (C=C) within the polymer chain, HCl release, crosslinking occurs, or sometimes chain scission depending on the intensity of the radiation. These changes can increase the number of charge carriers, leading to increased conductivity [21]. The results revealed that increased photodegradation was accompanied by

a rise in electrical conductivity, attributed to the creation of polyene, hydroxyl, and carbonyl groups within the polymer chain, indicating progressive chemical degradation.

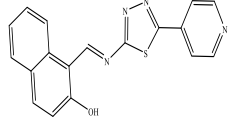
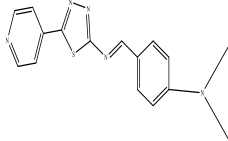
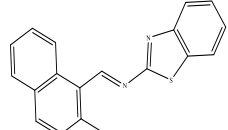
2. MATERIALS AND METHODS

A variety of chemicals, solvents, and reagents supplied by different commercial sources were utilized as the primary materials for conducting the experimental work. p-(Dimethylamino) benzaldehyde 99%, 5-(pyridin-4-yl)-1,3,4-thiadiazol-2-amine 99%, 2-hydroxy-1-naphthaldehyde 99%, 2-aminobenzothiazole 98%, PVC (98%), tetrahydrofuran (THF) (99%), and absolute ethanol were purchased from Merck Co. and used as received without further purification. Structural characterization was performed by Proton Nuclear Magnetic Resonance (¹H-NMR) spectroscopy employing an Avance Neo 400 instrument at the laboratories of Bagdad University. Complementary information regarding functional groups and molecular features was obtained through infrared spectroscopic analysis using an FTIR Perkin-Elmer spectrometer. The melting points of the final products were measured with a digital Stuart SMP10.

2.1 Synthesis of Schiff base

0.08 g (0.56 mmol) p-(Dimethylamino) benzaldehyde was dissolved in 10 mL of absolute ethanol in a 50 mL round-bottom flask. Two drops of concentrated hydrochloric acid were added as a catalyst, and the mixture was stirred at room temperature for 15 minutes. Afterward, 0.1 g (0.56 mmol) of 5-(pyridin-4-yl)-1,3,4-thiadiazol-2-amine, dissolved in 15 mL of absolute ethanol, was added slowly with continuous stirring. In this case, the reaction mixture was heated under reflux at 77 °C for 40 hours. Upon completion of the reaction, the majority of the solvent was evaporated using an oven maintained at 50 °C. The resulting solid red product was collected by filtration and purified by recrystallization from ethanol. The same synthetic procedure was applied using 0.10 g (0.66 mmol) of 2-hydroxy-1-naphthaldehyde and 0.10 g (0.66 mmol) of 2-aminobenzothiazole (Figure 1). The yields and selected physical properties of the synthesized compounds (M4, M9, and MM4) are listed in Table 1 [22].

Table 1. The codes, names, and structures of the compounds that were synthesized

Com. No.	Structural Formulation of Compounds	Names of Compounds
M4		1-(((5-(pyridin-4-yl)-1,3,4-thiadiazol-2-yl)imino)methyl)naphthalen-2-ol
M9		N,N-dimethyl-4-(((5-(pyridin-4-yl)-1,3,4-thiadiazol-2-yl)imino)methyl)aniline
MM4		1-((benzo[d]thiazol-2-yl)imino)methyl)naphthalen-2-ol

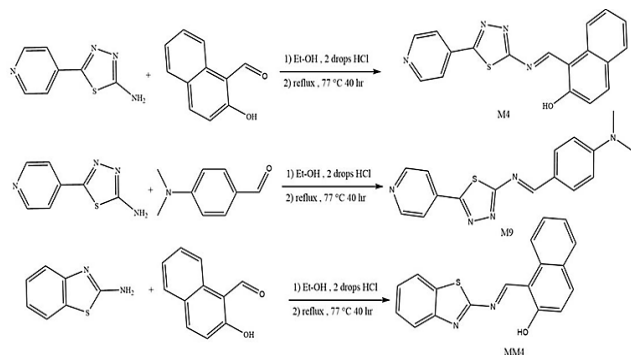


Figure 1. The diagram illustrates the synthesis of Schiff's bases

2.2 Method of preparing films

A 3% PVC solution was prepared by completely dissolving 3 grams of PVC in 100 mL of THF. Subsequently, 0.0067 g of Schiff base was added to 25 mL of the 3% PVC solution to achieve a 0.9% wt. concentration, resulting in a homogeneous mixture. The mixture was poured into glass molds and allowed to dry for 48 hours at 25 °C to prepare the films. After complete solvent evaporation and film drying, the films were detached from the molds and fixed onto 3 × 3 cm paper substrates [23]. The PVC films prepared were 40 μm thick, as measured using a micrometer, model 2610 (Germany).

2.3 Accelerated testing technique

The PVC films were subjected to irradiation for a duration of 300 h. using a rapid weathering meter (QUV) equipped with two 18 W UV-A lamps (365 nm). The distance between the samples and the lamps was maintained at 10 cm, the light intensity was maintained at 2.2×10^{-6} Ein·dm⁻³·s⁻¹ (18 W/m²), and the experiments were conducted at room temperature. This device simulates the effects of solar radiation to evaluate the resistance of materials to UV-induced degradation. The irradiation intensity was expressed in Einstein units (2.2×10^{-6} Ein·dm⁻³·s⁻¹), representing photon flux. For consistency with standard polymer photodegradation studies, this value corresponds approximately to 18 W/m² at 365 nm, taking into account photon energy and a film thickness of 40 μm [24, 25].

2.4 Measurement of photodegradation methods

The photodegradation of the PVC films was assessed using several techniques, with a primary focus on FTIR spectroscopy. This technique operates within the spectral range of 400 to 4000 cm⁻¹ and is instrumental in monitoring the photodegradation of both pure PVC films and those containing additives over varying irradiation durations. The carbonyl index (CI) was measured at 1724 cm⁻¹, which increases with prolonged irradiation, indicating photodegradation. This was referenced against the stable 1427 cm⁻¹ band, which remains comparatively stable under the same conditions using the CI method, allowing a quantitative assessment of degradation and insight into its mechanisms. The relationship between these bands can be expressed mathematically, as detailed in the accompanying Eq. (1).

$$I_s = \frac{A_s}{A_t} \quad (1)$$

In this context, let A_s represent peak absorbance of the sample during irradiation at 1724 cm⁻¹, while A_t represent the peak absorbance of the reference band at 1427 cm⁻¹, which remains constant before and after irradiation. The carbonyl index (I_s) can be calculated using these values. The absorbance (A) of the carbonyl band (C = O) of PVC is derived from the wavenumber using the following Eq. (2):

$$A = -\log_{10} \left(\frac{\%T}{100} \right) \quad (2)$$

In this context, %T represents the ratio of transmittance. The actual absorbance is calculated using the formula [26]:

$$A = A_{top\ band} - A_{base\ line}$$

In this method, the baseline is drawn tangent to the shoulder of the absorption band, as shown in Figures 2(A) and (B).

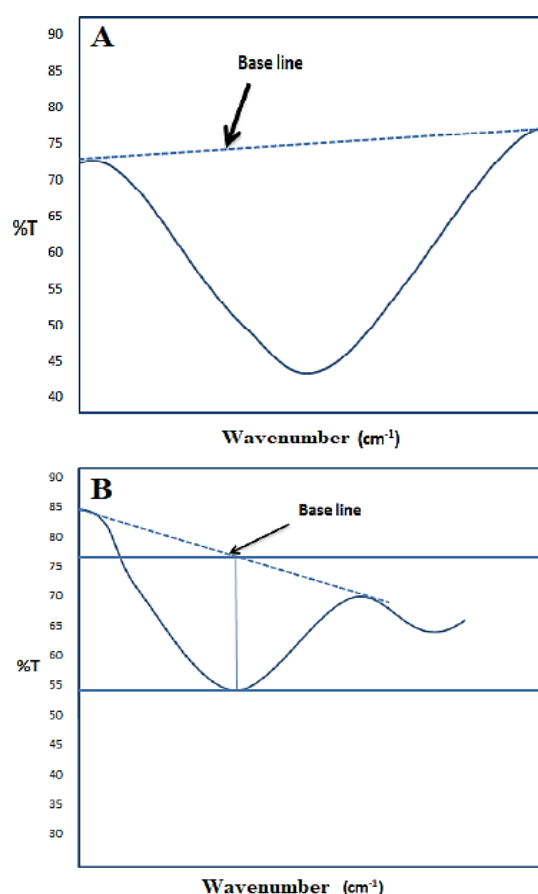


Figure 2. The characteristic absorption bands appearing in the FTIR spectra and demonstrates the method used for baseline selection during carbonyl index (CI) calculation

Figures 3 and 4 illustrate the calculations for the change in the infrared spectra of pure PVC with a thickness of 40 μm. The baselines selected based on the absorbance at wavenumber 1724 cm⁻¹ for the carbonyl group and wavenumber 1427 cm⁻¹ for the reference peak are shown. The carbonyl coefficient is then calculated based on the change in infrared spectra before and after irradiation, as detailed in Table 2. The CI was calculated based on single representative FTIR measurements for each sample, focusing on the chemical structural changes at the surface.

By applying Eq. (1), we obtain the CI.

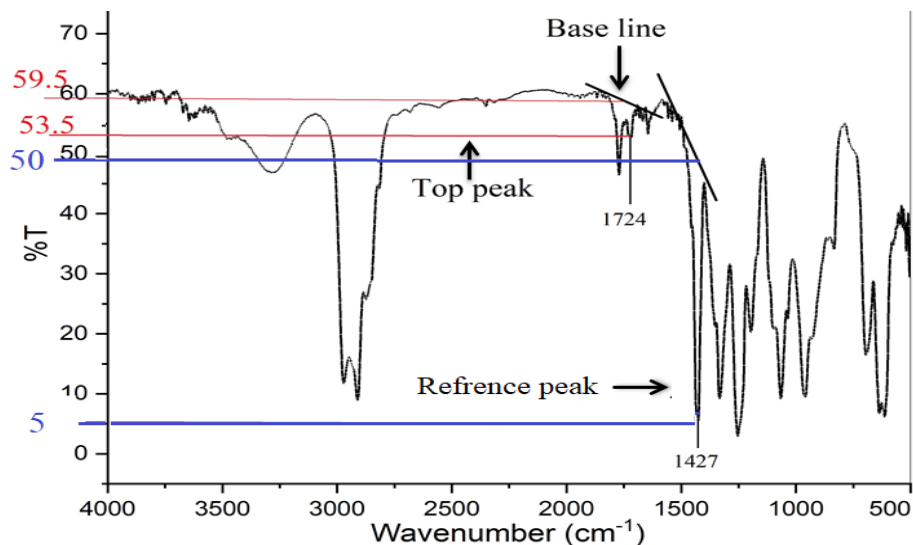


Figure 3. FTIR spectrum of pure PVC explains the top peak and baseline before irradiation with UV light
 Note: FTIR: Fourier Transform Infrared, PVC: polyvinyl chloride, UV: ultraviolet.

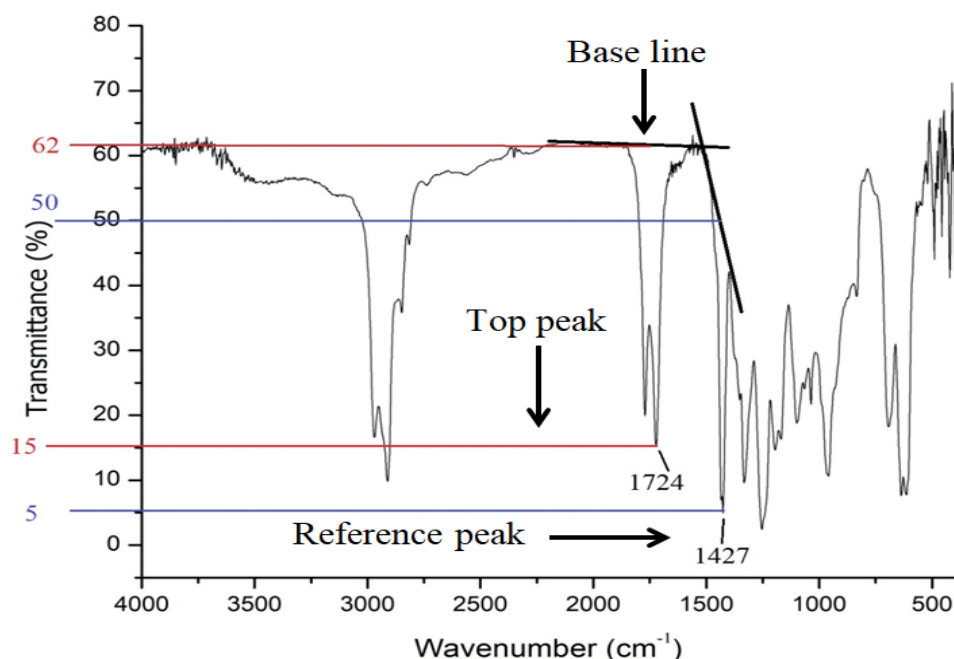


Figure 4. FTIR spectrum of pure PVC explains the top peak and baseline after 300 h irradiation with UV light
 Note: FTIR: Fourier Transform Infrared, PVC: polyvinyl chloride, UV: ultraviolet.

Table 2. Calculation of the carbonyl index (CI) at different irradiation times

Type of Band	Radiation Time (h)	Top Band		Base Line		The Actual Absorbance $A = A_{top} - A_{base\ line}$
		%T	$A = -\log_{10} \left(\frac{\%T}{100} \right)$	%T	$A = -\log_{10} \left(\frac{\%T}{100} \right)$	
Carbonyl C=O 1724	0	53.5	0.272	59.5	0.225	0.05
	300	15	0.823	62	0.207	0.616
Reference band	0	5	1.301	50	0.301	1
	300	5	1.301	50	0.301	1

2.5 Determination of viscosity average molecular weight (\overline{M}_v)

The viscosity average molecular weight \overline{M}_v provides valuable data about the estimated molecular weight of the polymer. This value is considered using the following Eq. (3):

$$[\eta] = K(\overline{M}_v)^\alpha \quad (3)$$

In this context, the parameters K and α represent constants characteristic of PVC under fixed temperature and solvent conditions. THF was employed as the solvent at 30 °C, with K and α values of 0.00015 and 0.77, respectively. The intrinsic viscosity $[\eta]$ was evaluated using a U-tube Ostwald viscometer

by measuring the flow times of the PVC solution (t) and the pure THF solvent (t_0). Viscosity values were subsequently calculated according to the following Eqs. (4)-(6) [27]:

$$\text{Relative viscosity } \eta_{rel} = \frac{t}{t_0} \quad (4)$$

$$\text{Specifically viscosity } \eta_{sp} = \frac{t}{t_0} - 1 \quad (5)$$

$$\text{Intrinsic viscosity } [\eta] = \sqrt{\left[\left(\frac{\sqrt{2}}{C}\right)(\eta_{sp} - \eta_{rel})\right]} \quad (6)$$

2.6 Ultraviolet-visible spectroscopic measurements

The UV-visible spectrophotometry method was employed to determine the photodegradation rate constant (k_d) of Schiff base additives at various irradiation times, specifically at the maximum absorption peak (λ_{max}). This wavelength corresponds to the increase in the carbonyl group concentration, which rises as the degree of Schiff base. k_d was calculated using the first-order kinetic equation:

$$\ln(A_t - A_\infty) = \ln(A_0 - A_\infty) - k_d t \quad (7)$$

The absorbance of the additive-containing PVC film before exposure to irradiation is denoted as A_0 , while A_t represents the absorbance recorded following a certain irradiation duration. A_∞ indicates the absorption at infinite irradiation time, and t is the irradiation time measured in seconds. Consequently, plotting $\ln(A_t - A_\infty) = \ln(A_0 - A_\infty)$ against the irradiation time (t) yields a straight line, with the slope corresponding to the photodegradation rate constant (k_d). This linear relationship demonstrates that the photodecomposition of PVC follows first-order kinetics [28].

2.7 The electrical characteristics

The electrical characteristics of the PVC films were analyzed using an LCR meter, which provides measurements of induction (L), capacitance (C), and resistance (R). These measurements were carried out across a frequency range of 5 Hz to 5 MHz at 25 °C, focusing on the alternating current electrical conductivity (σ_{AC}) of the films before and after UV exposure. When the films were irradiated at a wavelength of 365 nm with UV light, photodegradation occurred, resulting in the creation of carbonyl, polyene, and hydroxyl groups. These newly formed functional groups comprise lone electron pairs and partial charges, which enhance the electrical conductivity of the films. The observed increase in conductivity thus serves as a direct indication of the formation of these groups and confirms that photodegradation has occurred [29].

2.8 Determination of the quantum yield of polymer

The main-chain cleavage quantum yield (Φ_{cs}) was calculated to evaluate the polymer degradation efficiency based on molecular weight data derived from viscosity measurements. The calculations were performed using Eq. (8), taking into account Avogadro's constant, the concentration of added polymer, the intrinsic viscosity values before and after irradiation, as well as the exposure time and irradiation intensity. This coefficient indicates the efficiency of absorbed photons in inducing cleavage in the polymer chains, thus providing a deeper understanding of the mechanism

underlying the efficiency of photostabilization [30].

$$\Phi_{cs} = \left(\frac{C}{\bar{M}_{vo}}\right) \left[\frac{\left(\frac{[\eta_0]}{[\eta]}\right)^{\frac{1}{\alpha}} - 1}{I_o * t}\right] \quad (8)$$

where, C = concentrations (0.3 g/L), and $\alpha = 0.77$, \bar{M}_{vo} = the initial viscosity averages molecular weights, $[\eta_0]$ = Intrinsic viscosity before subjected to light, $[\eta]$ = intrinsic viscosity after subjected to light. I_o = the intensity of light used $2.2 \times 10^{-6} \frac{\text{Ein}}{\text{dm}^3 \cdot \text{s}}$, and t = time 300 h (1.08×10^6 seconds).

3. RESULTS AND DISCUSSIONS

3.1 Synthesis of Schiff bases

The physicochemical properties of the Schiff bases are shown in Table 3, and the spectral data for the synthesized derivatives are as follows [28]:

M4: 1-(((5-(pyridin-4-yl)-1,3,4-thiadiazol-2-yl)imino)methyl)naphthalen-2-ol: IR: band at 1603 cm^{-1} related to stretching of (C=N), broad band at 3090 cm^{-1} due to (OH) stretching, band at 1501 (C=C) aromatic stretching, 1314 (C-N stretching), 1245 (C-O stretching); $^1\text{H-NMR}$ (400 MHz, DMSO- d_6) $\delta = 14.99$ (1H, s, OH), 8.94 (1H, s, N=CH), 8.65-7.22 (10H, m, aromatic protons), which explains in the Figure 5.

M9: N, N-dimethyl-4-(((5-(pyridin-4-yl)-1,3,4-thiadiazol-2-yl)imino)methyl) aniline: IR: sharp band at 1652 cm^{-1} related to C=N stretching, 3039-2905 cm^{-1} (C-H aliphatic stretching), 1500 cm^{-1} (C=C stretching), 1371 cm^{-1} (C-N stretching), 1449 cm^{-1} (N-CH $_3$ bending); $^1\text{H-NMR}$ (400 MHz, DMSO- d_6) $\delta = 8.90$ (1H, s, N=CH), 8.65-6.77 (8H, m, aromatic protons), 3.03 (6H, s, N(CH $_3$) $_2$), as shown in Figure 6.

MM4: 1-((benzo[d]thiazol-2-ylimino)methyl)naphthalen-2-ol: IR: sharp band at 1653 cm^{-1} due to stretching of (C=N), broad band at 3555 cm^{-1} due to (OH stretching), 1510 (C=C stretching), 1323 (C-N stretching), 1250 (C-O stretching); $^1\text{H-NMR}$ (400 MHz, DMSO- d_6) $\delta = 14.99$ (1H, s, OH), 8.97 (1H, s, N=CH), 8.11-7.20 (10H, m, aromatic protons), as shown in Figure 7.

3.2 Prepared polyvinyl chloride films

The compounds (M4, MM4, and M9) were utilized as additives to enhance the photostability of PVC films. When the PVC films were exposed to UV radiation, bands appeared at 1772 cm^{-1} and 1724 cm^{-1} , indicating the creation of carbonyl groups associated with chloro ketone and aliphatic ketone compounds [31]. The FTIR spectrophotometer was employed to monitor the increase in the CI [32]. It was observed that by increasing the irradiation time, the carbonyl group increases. This increase in CI is attributed to the formation of carbonyl-containing oxidation products as a result of PVC photodegradation. Figure 8 illustrates the differences in the FTIR spectra of pure PVC before and after UV irradiation. As shown in Figure 8, the carbonyl content of the pristine polymer film increased after 300 hours of irradiation compared to the non-irradiated film, indicating photodegradation and the formation of ketone compounds. This highlights the need to incorporate stabilizing additives to

protect the polymer and mitigate its photodegradation under UV light exposure. And when the synthesis Schiff bases compounds (M4, MM4, and M9) were added as an additive to PVC polymer, and by scheming the CI after 300 h. irradiation, it was determined that the increase in the carbonyl group for the PVC with additive films was smaller than that observed in

the pure PVC film. The PVC film containing the M4 additive exhibited a lower increase in the CI compared to the supplementary composites, which can be attributed to its superior efficiency in suppressing the formation of carbonyl-containing degradation products. All of these additives functioned as photostabilizers for the PVC polymer.

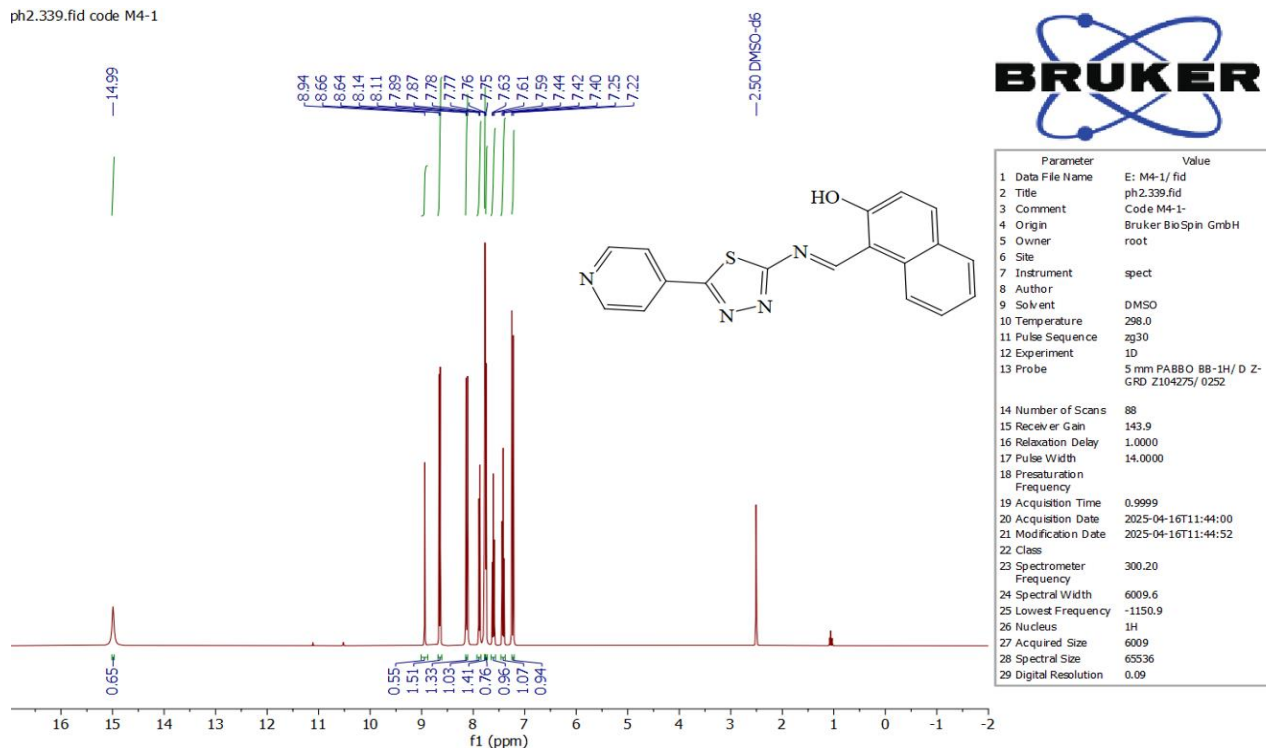


Figure 5. ¹H-NMR spectrum of M4 compound

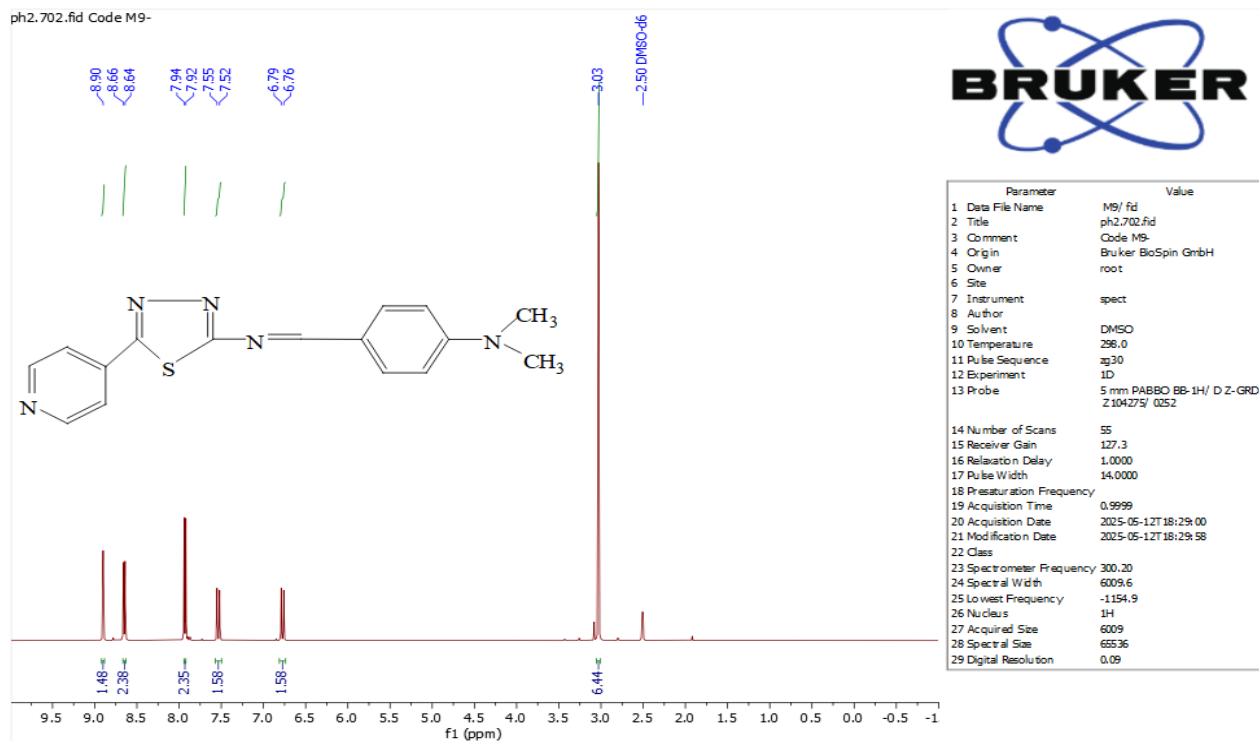


Figure 6. ¹H-NMR spectrum of M9 compound

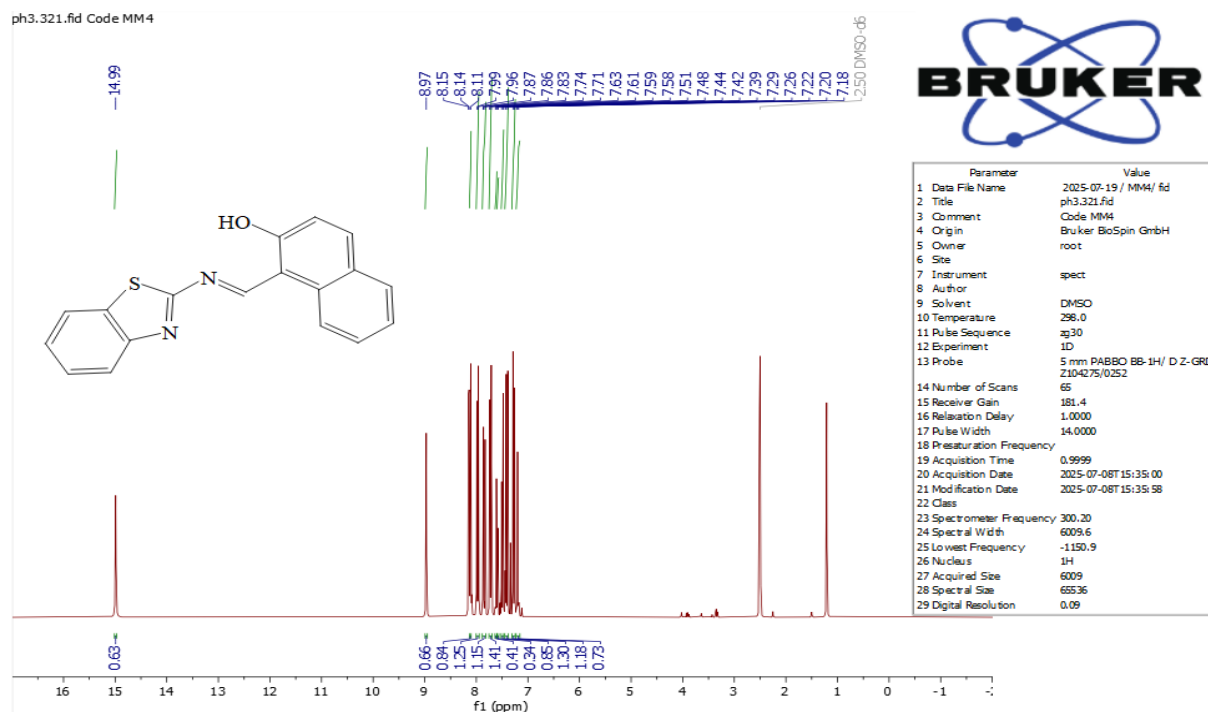


Figure 7. ¹H-NMR spectrum of MM4 compound

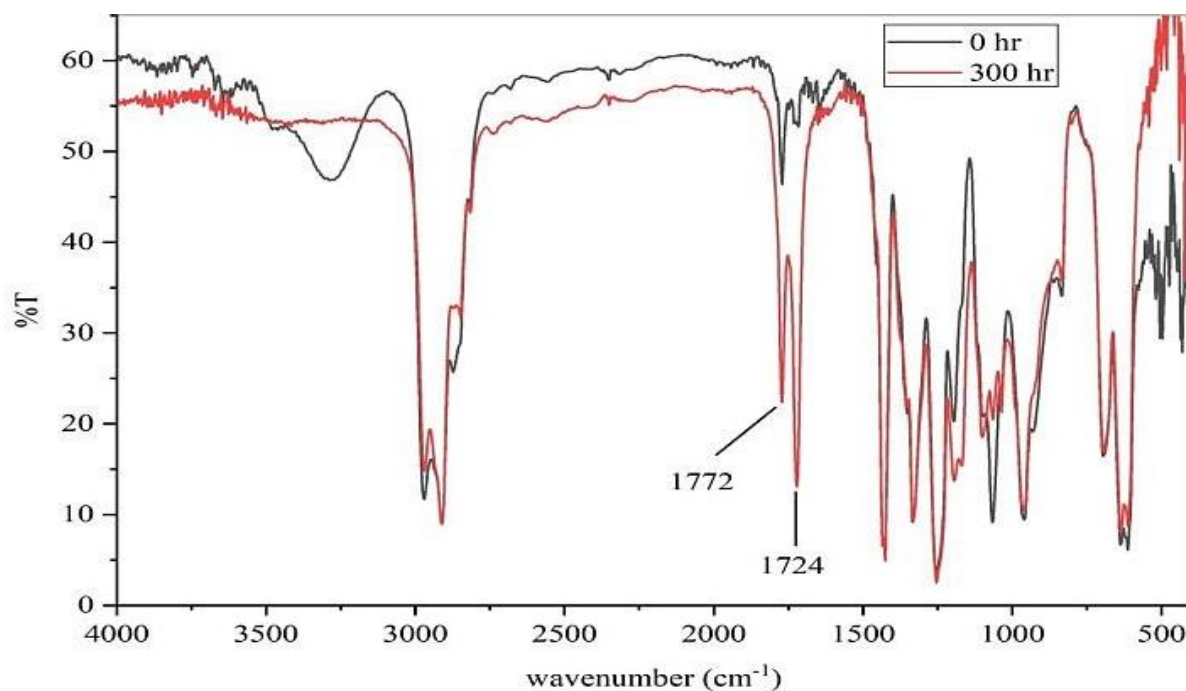


Figure 8. FTIR spectrum of pure PVC film before and after 300 h of exposure to UV radiation
 Note: FTIR: Fourier Transform Infrared, PVC: polyvinyl chloride, UV: ultraviolet.

Table 3. Physicochemical properties of the synthesized compounds

Com. No.	Molecular Formula	Molecular Weight (g/mol)	Melting Point (°C)	Color	Yield (%)
M4	C ₁₈ H ₁₂ N ₄ OS	332.38	154-156	yellow	54
M9	C ₁₆ H ₁₅ N ₅ S	309.39	209-211	red	36
MM4	C ₁₈ H ₁₂ N ₂ OS	304.37	178-180	yellow	42

3.3 Effect of additive concentration

The concentration of additives acting as photostabilizers plays a critical role in determining polymer stability. As reported in reference [33], increasing the additive content

leads to a noticeable decrease in the photodegradation rate of PVC, demonstrating enhanced resistance to light-induced deterioration. This indicates that higher additive concentrations effectively improve the polymer's photostability, with an optimal concentration of 0.9 wt%

providing the best compromise between compatibility, performance, and cost efficiency. Therefore, in the present study, the photostabilization of PVC was examined at an additive concentration of 0.9% weight, while maintaining a constant film thickness of 40 μm . Table 4 and Figure 9 illustrate the CI values calculated at different irradiation times for both the PVC control and the films containing additives (M4, M9, and MM4).

Table 4. Variation of the carbonyl index (CI) with irradiation time for PVC films of 40 μm thickness containing 0.9% additives M4, M9 and MM4

Additives Times	PVC (control)	M4	M9	MM4
0	0	0	0	0
50	0.1537	0.0905	0.1203	0.14
100	0.2358	0.117	0.1483	0.1794
150	0.3632	0.1447	0.1971	0.2311
200	0.4761	0.2084	0.2596	0.3327
250	0.5667	0.2469	0.3425	0.384
300	0.602	0.2711	0.3495	0.418

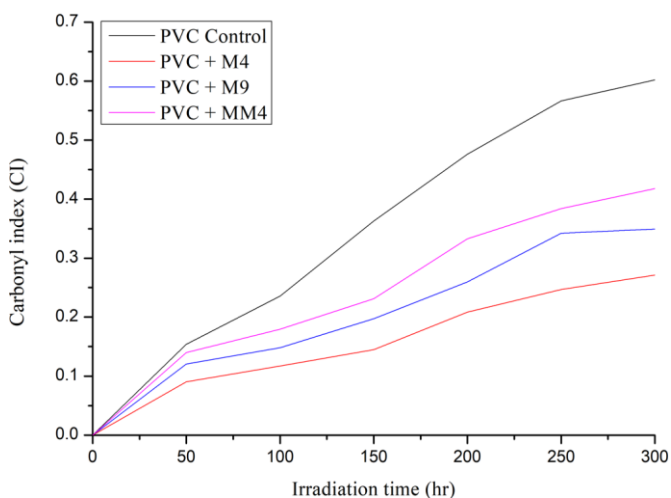


Figure 9. The association between carbonyl index (CI) and irradiation time (h) for pure PVC and PVC with additives films at a thickness of 40 μm
Note: PVC: polyvinyl chloride.

From Figure 9, it is evident that the additives exhibit a lesser increase in the CI compared to the PVC control over irradiation time. This suggests that these organic compounds function as photostabilizers for PVC against UV light at a wavelength of 365 nm, following the trend: M4 > M9 > MM4 > PVC. The superior performance of M4 may be attributed to its enhanced ability to suppress the formation of carbonyl-containing degradation products. While the current study relies on single measurements per sample point, which is common in many FTIR-based polymer degradation studies, we acknowledge that further statistical replicates could provide a more detailed map of surface heterogeneity.

The photodecomposition rate constant (k_d) for Schiff base as additives for PVC were planned using Equivalence 7, based on the changes in UV spectra of prepared films. This reaction is first-order, and the diagram of $\ln(A_t - A_\infty)$ in contradiction to irradiation time yields a traditional line. The slope of this line represents (k_d) (see Table 5) [34].

The UV-Vis spectra showed absorption maxima around 320 nm for M4 and M9, while MM4 exhibited a bathochromic shift

due to its higher degree of conjugation, which also explains the observed color differences, as shown in Figures 10(A-C) [35].

Table 5. Photodecomposition rate constants (k_d) for polyvinyl chloride (PVC) with M4, M9, and MM4 compounds

Sample	Photodecomposition Rate Constant (k_d) (s^{-1})	λ_{max} (nm)
PVC with M4	8.06×10^{-3}	319
PVC with M9	8.5×10^{-3}	324
PVC with MM4	9.2×10^{-3}	426
PVC (Control)	9.02×10^{-3}	273

The bathochromic shift observed for compound MM4 (426 nm) compared to the UV absorption of M4 and M9 is primarily attributed to the extended π -conjugation provided by the fused-ring system of the benzothiazole moiety, which significantly narrows the HOMO–LUMO energy gap.

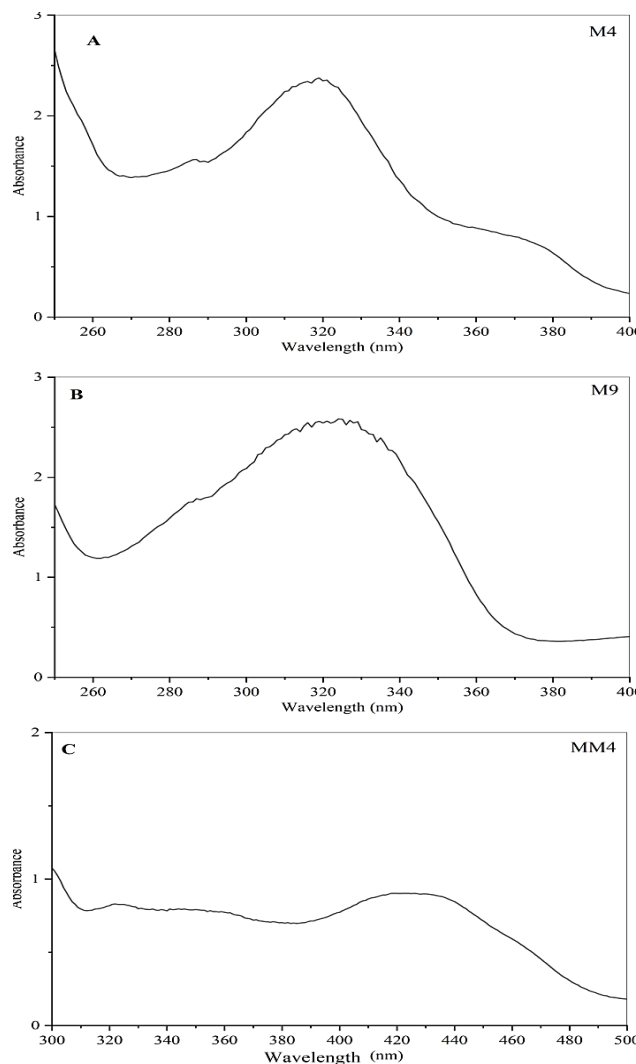


Figure 10. Ultraviolet (UV)-visible for (A) M4, (B) M9, and (C) MM4 compounds

While the ortho-hydroxyl group is present in both M4 and MM4, the benzothiazole system in MM4 facilitates a more rigid and planar molecular geometry. This structural rigidity

enhances the efficiency and stability of the intramolecular hydrogen bonding, providing greater stabilization of the excited state compared to the thiazazole derivatives. In contrast, the absence of this hydroxyl group in M9 further limits such stabilization. Collectively, these factors in MM4 synergistically facilitate electronic transitions at lower energy, shifting the absorption maximum into the visible region.

The PVC film containing the M4 additive exhibits a lower photodecomposition rate constant (k_d) value compared to other compounds. This indicates that the addition of the M4 compound enhances the photostability of the PVC film towards UV light, preventing significant degradation. The lower k_d value for the PVC with M4 additive film demonstrates that the M4 compound acts as an effective photostabilizer, protecting the PVC from UV-induced degradation and maintaining the polymer's molecular weight to a greater extent compared to the PVC control. When the pure PVC and PVC with additives compound films are exposed to UV radiation, the viscosity average molecular weight \overline{M}_v decreases with increasing irradiation time. This suggests that the irradiation causes chain scission, leading to a decrease in the regular molecular weight of the polymer [36] Table 6 and Figure 11 shows that the decrease in \overline{M}_v for both PVC control and PVC with additives is due to chain scission at multiple sites along the polymer backbone upon irradiation.

The PVC + M4 polymer film exhibited a high molecular weight even with prolonged irradiation time compared to other composite films, demonstrating its superior photostabilization efficiency. The electrical properties of pure PVC and PVC with M4 films, before and after irradiation, were confirmed using an LCR-meter model LCR-8105G industrial by GW Instek, with a frequency series of 5 Hz to 5 MHz at 25 °C and 1 atm. The data are presented in Tables 7 and 8. Figure 12 shows that at the initial stage, before any UV exposure, both

pure PVC and PVC with additive films display low electrical conductivity. This is due to the polymer chains remaining intact, which limits ion generation and restricts ion mobility within the polymer chain. As seen in Figure 13, increasing the irradiation time leads to a rise in AC electrical conductivity (σ_{AC}) for the pure PVC as well as for films containing M4, M9, and MM4 additives. This increase reflects the photodegradation of PVC, which results in the formation of this, due to the polymer chains remaining intact, which limits ion generation and restricts ion mobility within the polymer chain. As seen in Figure 9, increasing the irradiation time leads to a rise in AC electrical conductivity (σ_{AC}) for the pure PVC as well as for films containing M4, M9, and MM4 additives. carbonyl, polyene, and hydroxyl groups. These groups, possessing lone electron pairs and partial charges, enhance the material's conductivity. Notably, the PVC film with the M4 additive shows lower conductivity than the PVC control, indicating that the M4 compound (Schiff base) helps protect the polymer from degradation. This confirms the photostabilizing effect of M4 on PVC.

Table 6. Variation of the viscosity average molecular weight with irradiation time for PVC films of 40 μm thickness containing 0.9% additives M4, M9, and MM4

Additives Times	PVC (control)	M4	MM4	M9
0	160165	165778	161273	163992
50	125958	158836	142737	149740
100	118063	149825	131476	138648
150	108583	139398	122479	129478
200	101964	128957	113864	118479
250	95269	117726	103865	108585
300	87171	106127	92039	101520

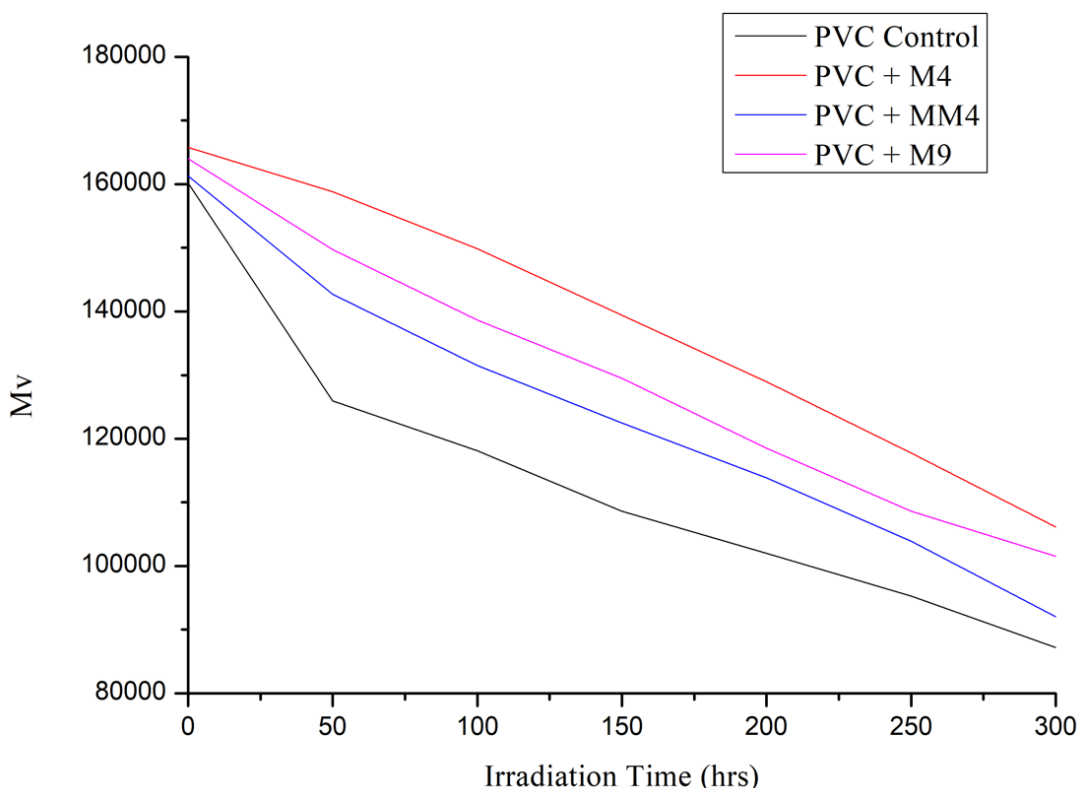


Figure 11. The decrease in \overline{M}_v of pure PVC and PVC with additives
Note: PVC: polyvinyl chloride.

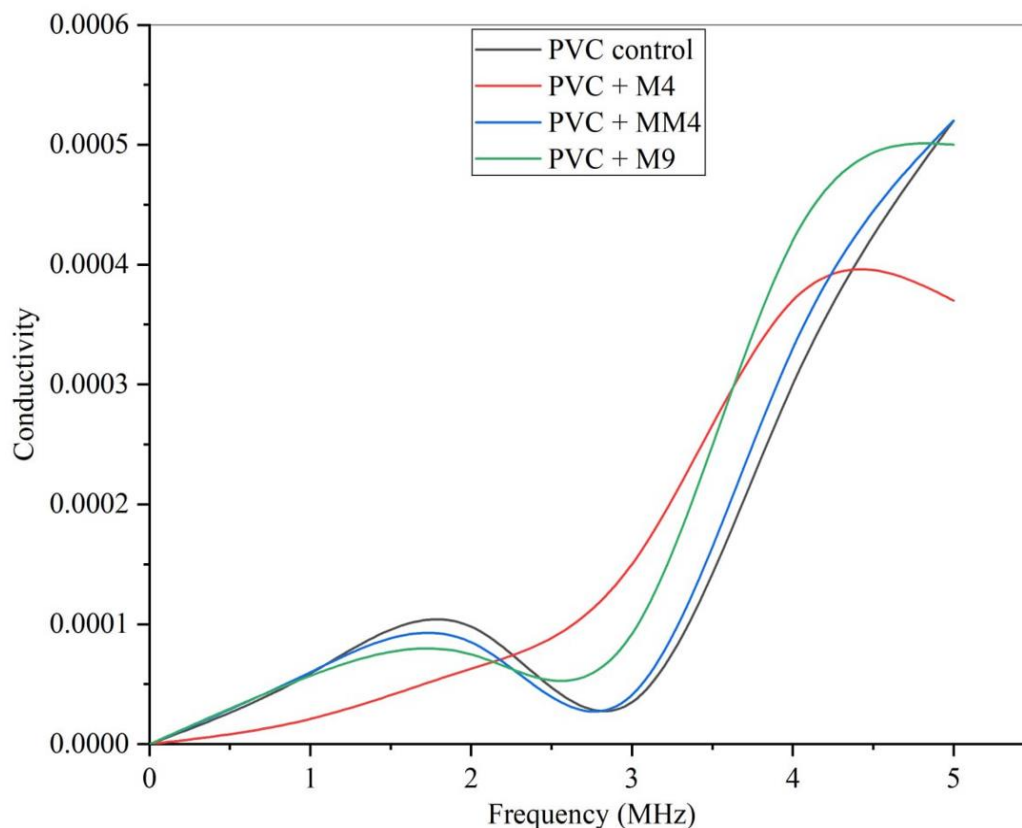


Figure 12. The conductivity of pure PVC and PVC with additives films before irradiation
Note: PVC: polyvinyl chloride.

Table 7. Electrical conductivity values of synthesized compounds as a function of frequency before irradiation

Frequency (MHz)	Conductivity (σ_{AC})			
	PVC Control	PVC + M4	PVC + MM4	PVC + M9
0	0	0	0	0
1	5.9×10^{-5}	2.1×10^{-5}	6×10^{-5}	5.7×10^{-5}
2	9.8×10^{-5}	6.3×10^{-5}	8.5×10^{-5}	7.5×10^{-5}
3	3.5×10^{-5}	1.5×10^{-4}	4.1×10^{-5}	9.2×10^{-5}
4	3×10^{-4}	3.7×10^{-4}	3.3×10^{-4}	4.2×10^{-4}
5	5.2×10^{-4}	3.7×10^{-4}	5.2×10^{-4}	5×10^{-4}

Note: PVC: polyvinyl chloride.

Table 8. Electrical conductivity values of synthesized compounds as a function of frequency after irradiation

Frequency (MHz)	Conductivity (σ_{AC})			
	PVC Control	PVC + M4	PVC + MM4	PVC + M9
0	0	0	0	0
0.5	7.23×10^{-5}	5.2×10^{-5}	4.25×10^{-5}	7.3×10^{-5}
1	1.09×10^{-4}	9.7×10^{-5}	8.2×10^{-5}	1.13×10^{-4}
2	2.69×10^{-4}	3.6×10^{-5}	1.7×10^{-5}	3.2×10^{-5}
3	4.36×10^{-4}	2.9×10^{-4}	2.8×10^{-4}	3.1×10^{-4}
4	5.01×10^{-4}	3.4×10^{-4}	3.7×10^{-4}	4.1×10^{-4}
5	6.22×10^{-4}	4.9×10^{-4}	4.6×10^{-4}	4.6×10^{-4}

Note: PVC: polyvinyl chloride.

From the above data, the percentage reduction based on the data presented in Table 8, the percentage reduction in the electrical conductivity (σ_{AC}) for the PVC + M4 composite was calculated after irradiation by using Eq. (9).

$$\text{Percentage reduction} = \left(\frac{\sigma_{PVC} - \sigma_{PVC+M4}}{\sigma_{PVC}} \times 100 \right) \quad (9)$$

The percentage reduction in conductivity for the PVC + M4

was found to be 21.2% at a frequency of 5 MHz after irradiation. This reduction is attributed to the role of M4 in enhancing the dielectric properties of the polymer. As an effective photostabilizer, M4 acts by inhibiting the generation of free radicals and charged species during the irradiation process, thereby limiting charge mobility and maintaining the insulating integrity of the PVC.

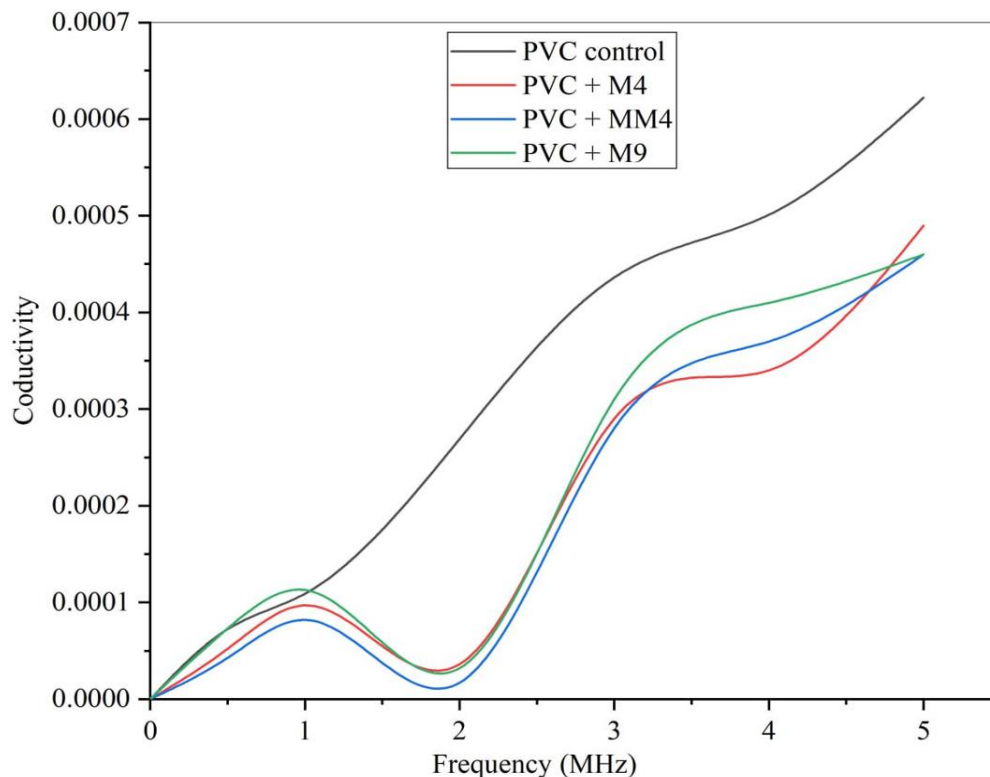


Figure 13. The conductivity of pure PVC and PVC with additives films after 300 h irradiation time
Note: PVC: polyvinyl chloride.

3.4 FESEM analysis of the surface morphology of prepared films

The consequence of UV light on the morphology of pure PVC and PVC with additives was investigated using field emission scanning electron microscopy. FESEM was used to study the morphology of the prepared PVC films, which provided an influential technique to characterize the shape and particle size changes. Figure 14 shows the FESEM images of prepared PVC films after 300 hours of UV irradiation. The figure shows that, before irradiation, the surface of pure PVC exhibits no cracks or pores. After irradiation, however, grooves and pores are observed [37]. These holes are likely the result of a high rate of HCl elimination during the irradiation process, indicating that the polymer was affected by UV radiation. In contrast, the surface of the additive-containing polymer after irradiation shows a lower degree of degradation, due to the action of the photostabilizers, which preserve the polymer structure from degradation [37]. In summary, the FESEM analysis provides insights into the morphological changes experienced by the pure and organically modified PVC films upon exposure to UV irradiation, including surface roughening and the formation of circular holes due to HCl elimination [38].

Based on the previous measurements and analyses using FTIR, UV-Visible spectroscopy, \bar{M}_v , LCR-meter, the M4 compound has demonstrated higher photostabilization performance compared to the other additives, with the following trend: M4 > M9 > MM4 > PVC.

Several mechanisms of photostabilization have been proposed to explain the observed results, such as primary stabilizer, UV absorber, and radical scavenger [39]. In the primary stabilizer, the Schiff base compounds can absorb the UV light and dissipate the absorbed energy in the form of harmless heat, preventing the polymer from undergoing

photodegradation [40]. In UV absorber, the Schiff base additives can effectively absorb the harmful UV radiation, shielding the PVC polymer from direct exposure and degradation. The Schiff base compounds in the radical Scavenger mechanism can intercept and neutralize the free radicals generated during the photodegradation process, thereby inhibiting the chain reactions that lead to polymer degradation [41]. Internal conversion (IC) and intersystem crossing (ISC) mechanisms [42]. Both IC and ISC play a crucial role in photostabilization by converting harmful UV energy into thermal energy, thereby preventing photochemical degradation. These mechanisms are especially important in UV-absorbing additives and photostabilizers used for polymer protection, such as PVC [43]. This is shown in Figures 15 and 16.

The combination of these photostabilization mechanisms, with the M4 compound exhibiting the most effective performance, explains the superior photostability of the PVC films containing the M4 additive compared to the other formulations and the PVC control. The superior photostabilizing performance of M4 compared to the MM4 is driven by three structural advantages:

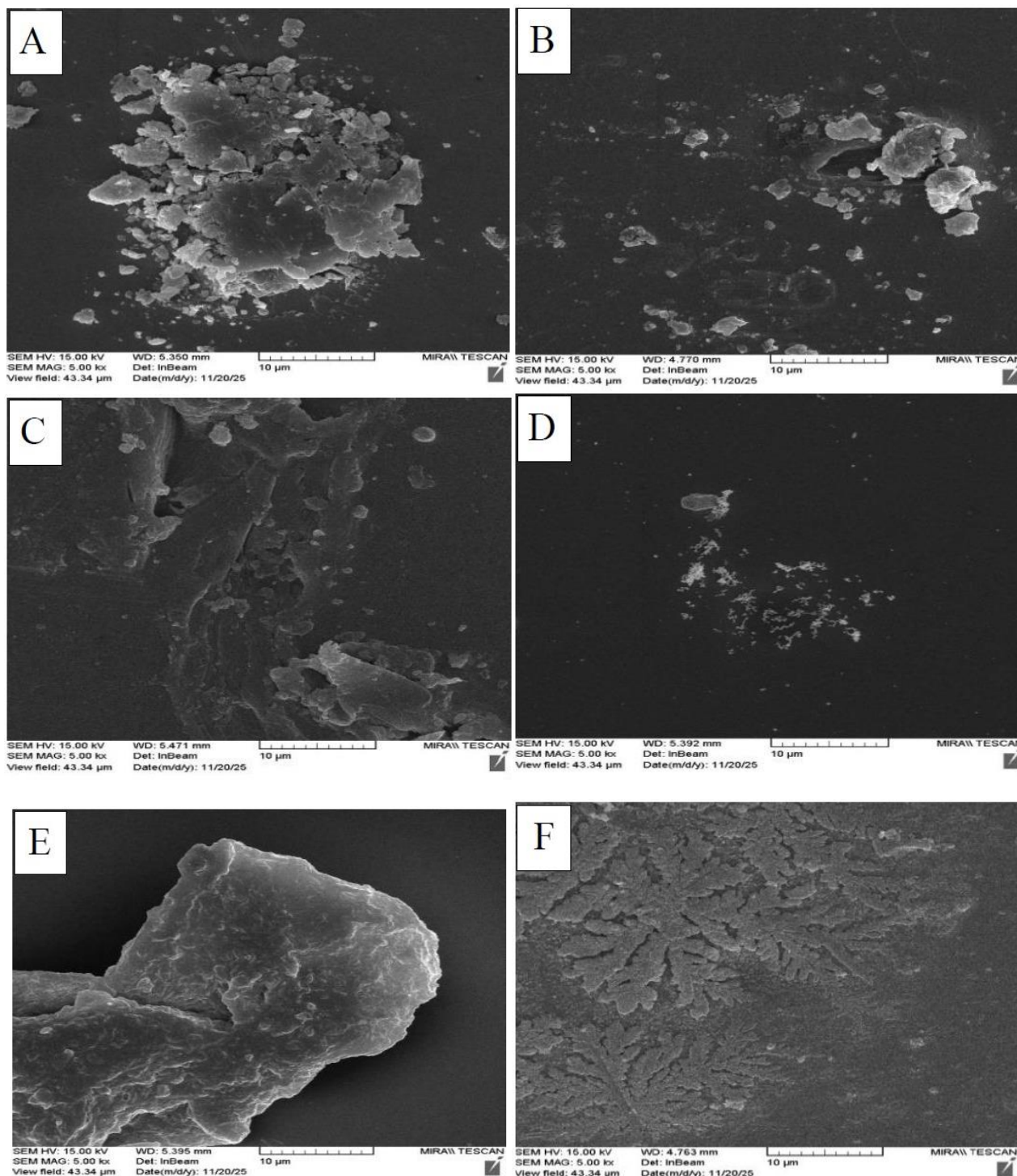
1. **Enhanced Matrix Compatibility:** The incorporation of the pyridine moiety increases the molecule's polarity, leading to better dispersion and homogeneity within the polar PVC.

2. **Optimized Energy Dissipation:** The pyridine-thiazole architecture provides a more versatile electronic configuration than the naphthalene-benzothiazole system. This allows for a more efficient dissipation of absorbed UV energy across a broader spectral range, preventing local photochemical damage.

3. **Synergistic Radical Scavenging:** The nitrogen-rich heterocycle acts as an effective radical scavenger and potential metal chelator, actively neutralizing the free radicals and catalytic metallic impurities that drive the photo-oxidative

degradation of the PVC chains. whereas the lower efficiency of MM4 may be due to steric hindrance and reduced dispersion. The Schiff base additives demonstrate superior photostabilizing performance for PVC through a combination of five key mechanisms: Primary Stabilizer Mechanism: M4 interacts with PVC chains through hydrogen bonding and electrostatic interactions between its heteroatoms (N and S) and the partially positive carbon atoms in the PVC backbone. These interactions reduce polymer chain mobility, suppress HCl elimination, and inhibit radical formation, thereby improving the thermal and photostability of PVC [40], which shown in Figure 17. In the UV absorber mechanism, M4 absorbs UV radiation due to its extended conjugated aromatic system. Upon UV absorption, the molecule is excited to a

higher electronic state and then releases the absorbed energy through non-radiative processes such as IC and proton transfer. The excess energy is dissipated as heat, preventing UV radiation from reaching and degrading the PVC chains [41], which explains in Figure 18. In the radical Scavenger mechanism: During thermal or photo-degradation of PVC, reactive free radicals and peroxy radicals (such as $\text{POO}\cdot$) are formed. M4 reacts with these radicals by donating a hydrogen atom or an electron from its phenolic group or conjugated system, converting them into more stable species. The resulting M4 radical is resonance-stabilized, which terminates the radical chain reactions responsible for PVC degradation [42]. Therefore, this mechanism is sometimes referred to as secondary stabilizers, which is explained in Figure 19.



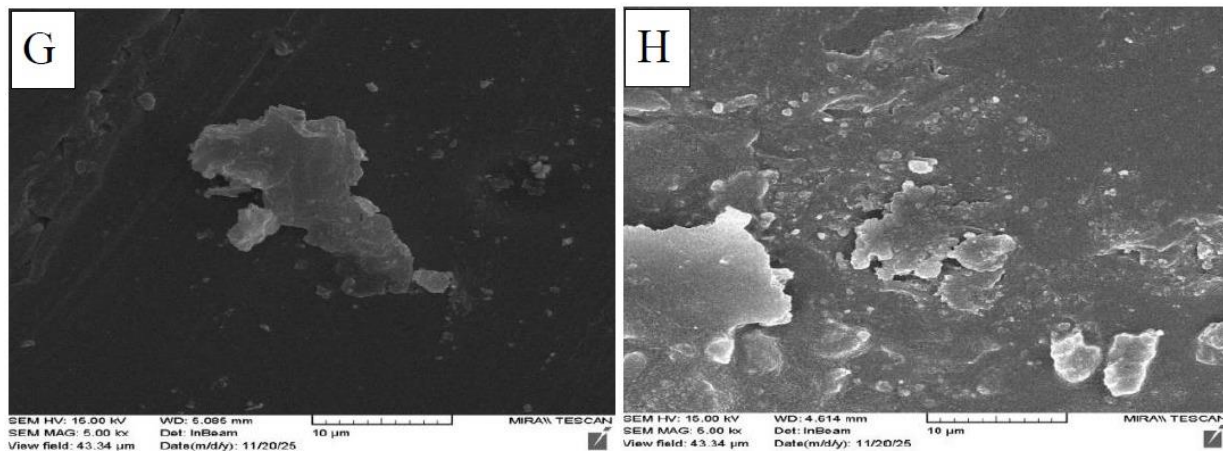


Figure 14. FESEM images: Pure PVC (A) before irradiation, (B) after irradiation, PVC + M4 (C) before irradiation, (D) after irradiation, PVC + M9 (E) before irradiation, (F) after irradiation, and PVC + MM4 (G) before irradiation, (H) after irradiation
Note: PVC: polyvinyl chloride.

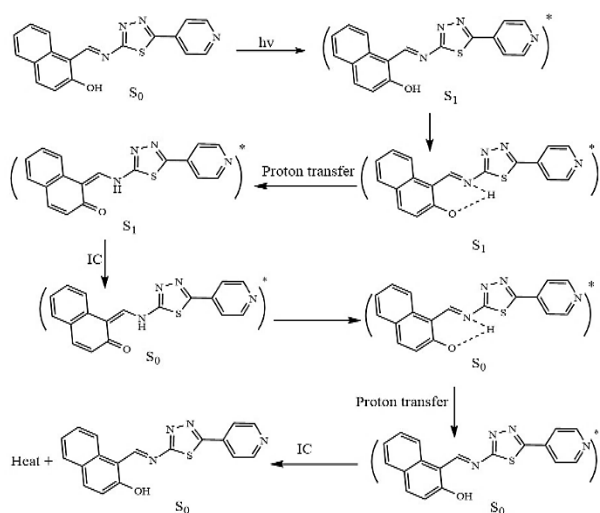


Figure 15. The proposed mechanism for polyvinyl chloride (PVC) photostabilization by the M4 compound involves internal conversion (IC)

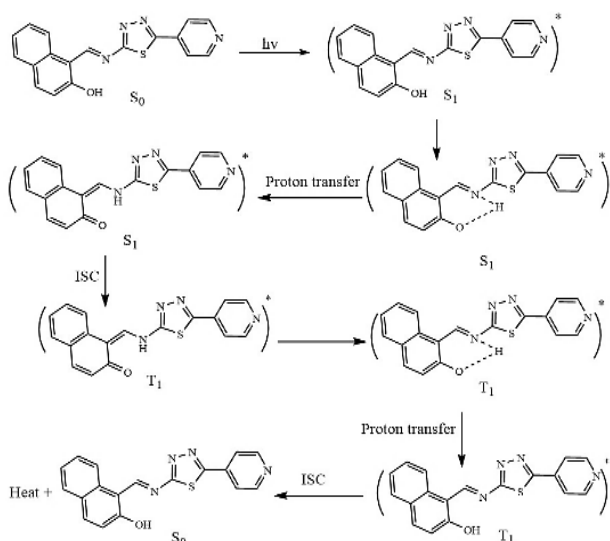


Figure 16. The proposed mechanism for polyvinyl chloride (PVC) photostabilization by the M4 compound involves intersystem crossing (ISC)

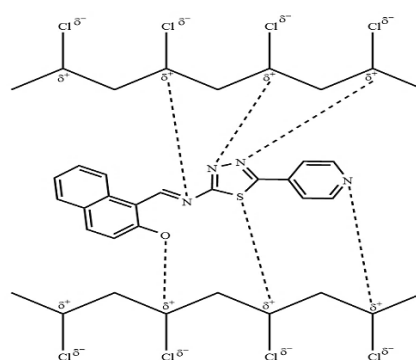


Figure 17. The proposed mechanism for polyvinyl chloride (PVC) photostabilization by the M4 compound involves a primary stabilizer

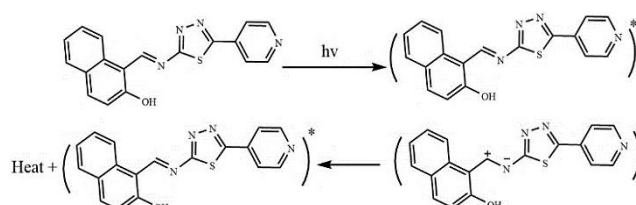


Figure 18. The proposed mechanism for polyvinyl chloride (PVC) photostabilization by the M4 compound involves the ultraviolet (UV) absorber

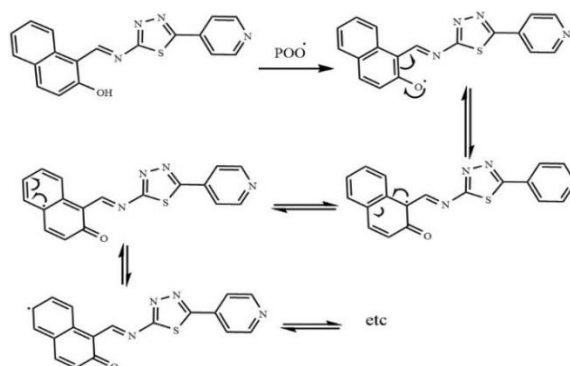


Figure 19. The proposed mechanism for polyvinyl chloride (PVC) photostabilization by the M4 compound involves a radical scavenger

The synergistic effect of these five mechanisms explains the superior photostabilizing performance of the M4 Schiff base additive compared to the other formulations.

3.5 Quantum yield analysis

The characterization of the degradation reaction can be understood by calculating the quantum yield of chain scission (Φ_{cs}). This value was calculated for both pure PVC and PVC containing 0.9% (wt./wt.) of the additives (M4, M9, and MM4). The resulting Φ_{cs} values at similar irradiation times are presented in Table 9. The Φ_{cs} value for PVC with M4 film is lower than that of M9, with the order being MM4 < pure PVC (control). The observed reductions in quantum yield in the presence of the additive are likely due to the delocalization of absorbed energy within the PVC during irradiation. Energy absorbed at a single site tends to be distributed across multiple bonds, which decreases the likelihood of bond cleavage. Furthermore, some of the absorbed energy may be dissipated or redirected through non-reactive pathways, resulting in a decrease in overall photochemical efficiency [44, 45]. This suggests that PVC with M4 exhibits greater resistance to degradation, thereby better preserving the PVC components from deterioration.

While the synthesized Schiff bases demonstrated significant photostabilization efficiency and effectively reduced the rate of PVC degradation compared to the pristine polymer, we acknowledge that their performance may not yet reach the optimized levels of specialized commercial stabilizers like HALS. The primary objective of this study was to explore the fundamental mechanism and efficiency of these new Schiff bases as intrinsic stabilizers. A comparative performance profile suggests they are promising candidates, and although a side-by-side experimental benchmark with HALS was not within the initial scope, this provides a clear pathway for future optimization of these derivatives.

Table 9. Quantum yield (Φ_{cs}) for chain scission of pure polyvinyl chloride (PVC), M4, M9, and MM4 films after 300 h irradiation time

Sample	Quantum Yield of Main Chain Scission (Φ_{cs})
PVC	6.69×10^{-7}
PVC with M4 Compound	4.75×10^{-7}
PVC with M9 Compound	5.00×10^{-7}
PVC with MM4 Compound	6.16×10^{-7}

4. CONCLUSION

Three new aromatic Schiff base compounds (M9, M4, and MM4) were synthesized, characterized and evaluated as photostabilizers for PVC. The PVC control film and PVC with additive films containing 0.9 %wt. showed photostabilization efficiency in the order: M4 > M9 > MM4 > PVC control. The PVC with M4 film exhibited a lower CI increase, indicating a high photostability, which is attributed to its high compatibility with the PVC chain and effective engagement in multiple photostabilization mechanisms. Due to their excellent stability under UV light, these Schiff base compounds act as highly efficient photostabilizers for PVC, effectively

suppressing the liberation of (HCl) hydrochloric acid, that work as the primary driver of polymer degradation of free radical after liberate from PVC backbone. This protection is achieve through several mechanisms include primary stabilizers, absorbing harmful UV radiation, and free radicals scavenger that can damage the polymer chains. And dissipate the absorbed harmful energy through IC and ISC. The efficiency of these additives was visually proved by FESEM analysis, which revealed that PVC with additive films preserved a significantly smoother surface morphology with minimal crack formation post irradiation compared to the pure polymer. Among the synthesized candidates, compound M4 exhibited the most prominent photostabilizing efficiency, highlighting the potential of highly aromatic Schiff bases in expanding the outdoor durability of PVC materials.

ACKNOWLEDGMENT

The authors wish to thank the Department of Chemistry at the Colleges of Science in Diyala and Samarra Universities for their valuable support and for making the Polymer Research Unit facilities available for this work.

REFERENCES

- [1] Tulane, R.S., Afonso, R.G., Daiane, C., Markssuel, T.M., Mugahed, A., Roman, F., Nikolai, V., Maria, K., Sergey, K., Maciej, S. (2021). Application of plastic wastes in construction materials: A review using the concept of life-cycle assessment in the context of recent research for future perspectives. *Materials*, 14(13): 3549. <https://doi.org/10.3390/ma14133549>
- [2] Krzysztof, L., Katarzyna, S. (2022). A brief review of poly (vinyl chloride)(PVC) recycling. *Polymers*, 14(15): 3035. <https://doi.org/10.3390/polym14153035>
- [3] Huang, Z., Ding, A., Guo, H., Lu, G.L., Huang, X.Y. (2016). Construction of nontoxic polymeric UV-absorber with great resistance to UV-photoaging. *Scientific Reports*, 6(1): 25508. <https://doi.org/10.1038/srep25508>
- [4] Farhan, M.A., Al-Garawi, Z.S., Ali, W.B., Nief, O.A. (2023). A novel method for long-term preserving of urine microstructure using poly (vinyl chloride). *Journal of Applied Polymer Science*, 140(26): e54000. <https://doi.org/10.1002/app.54000>
- [5] Chamas, A., Moon, H., Zheng, J.J., Qiu, Y., Tabassum, T., Jang, J.H., Abu-Omar, M., Scott, S.L., Suh, S. (2020). Degradation rates of plastics in the environment. *ACS Sustainable Chemistry & Engineering*, 8(9): 3494-3511. <https://doi.org/10.1021/acssuschemeng.9b06635>
- [6] Arraq, R.R., Hadi, A.G., Ahmed, D.S., El-Hiti, G.A., Kariuki, B.M., Husain, A.A., Bufaroosha, M., Yousif, E. (2023). Enhancement of photostabilization of poly (vinyl chloride) in the presence of tin-cephalexin complexes. *Polymers*, 15(3): 550. <https://doi.org/10.3390/polym15030550>
- [7] Ennadafy, H., Jammoukh, M., Hilali, Y., Belouaggadia, N. (2024). Thermogravimetric analysis of rigid PVC and animal-origin bio-composite: Experimental study and comparative analysis. *International Journal of Heat and Technology*, 42(1): 39-49. <https://doi.org/10.18280/ijht.420105>

- [8] Soliman, S.M., Sanad, M.A., El-Ghaffar, M.A.A., Abdelwahab, N.A., Sabaa, M.W. (2025). Investigating ortho, meta, and para polytoluidine derivatives: Applications in photostabilization of PVC. *Chemistry Africa*, 8: 4865-876. <https://doi.org/10.1007/s42250-025-01464-0>
- [9] Yaqoob, A.A., Mohd Noor, N.H.B., Serra, A., Mohamad Ibrahim, M.N. (2020). Advances and challenges in developing efficient graphene oxide-based ZnO photocatalysts for dye photo-oxidation. *Nanomaterials*, 10(5): 932. <https://doi.org/10.3390/nano10050932>
- [10] Ma, L.J., Lu, Y.H., Chen, Y., Lu, Y.W., Yuan, G. (2022). Dehydrochlorination study of plasticized poly (vinyl chloride) containing modified titanium dioxide, cerium stearate, organotin and β -diketone complex after long-term storage. *Materials Research Express*, 9(2): 025305. <https://doi.org/10.1088/2053-1591/ac4f87>
- [11] Ghaedi, M., Niknam, E. (2010). Application of Triton X-100 Coated Poly Vinyl Chloride as new solid phase for Preconcentration of Fe³⁺, Cu²⁺ and Zn²⁺ Ions and their flame atomic absorption spectrometric determinations. *Bulletin of the Chemical Society of Ethiopia*, 24(1): 11-20. <https://doi.org/10.4314/bcse.v24i1.52956>
- [12] Chai, R.D., Zhang, J. (2013). Synergistic effect of hindered amine light stabilizers/ultraviolet absorbers on the polyvinyl chloride/powder nitrile rubber blends during photodegradation. *Polymer Engineering & Science*, 53(8): 1760-1769. <https://doi.org/10.1002/pen.23432>
- [13] Xue, M.Y., Lu, Y.H., Li, K., Wang, B., Lu, Y.W. (2020). Thermal characterization and kinetic analysis of polyvinyl chloride containing Sn and Zn. *Journal of Thermal Analysis and Calorimetry*, 139(2): 1479-1492. <https://doi.org/10.22146/ajche.19436>
- [14] Wang, B., Lu, Y.H., Lu, Y.W. (2020). Organic tin, calcium-inc and titanium composites as reinforcing agents and its effects on the thermal stability of polyvinyl chloride. *Journal of Thermal Analysis & Calorimetry*, 142(2): 71-683. <https://doi.org/10.1007/s10973-020-09767-9>
- [15] Stasac, C.O., Tomșe, A.D., Costea, T.O., Bandici, L., Arion, M.N., Hathazi, F.I. (2025). Accelerated aging process of carbon black-reinforced PVC (CB-PVC) insulation by UVB-induced chemical degradation. *Processes*, 13(6): 1844. <https://doi.org/10.3390/pr13061844>
- [16] Meng, J., Xu, B., Liu, F., Li, W., Sy, N., Zhou, X., Yan, B. (2021). Effects of chemical and natural ageing on the release of potentially toxic metal additives in commercial PVC microplastics. *Chemosphere*, 283: 131274. <https://doi.org/10.1016/j.chemosphere.2021.131274>
- [17] Elgamasy, S.M., Abd-ElRazek, S.E. (2023). Binuclear transition metal complexes containing schiff base ligand: Synthesis, characterization and microbicide activities. *Bulletin of the Chemical Society of Ethiopia*, 37(4): 901-915. <https://doi.org/10.4314/bcse.v37i4.8>
- [18] Farhan, M.A., Nief, O.A., Ali, W.B. (2022). New photostabilizers for poly (vinyl chloride) derived from heterocyclic compounds. *Eurasian Chemical Communications*, 4(6): 525-543. <https://doi.org/10.22034/ecc.2022.332467.1347>
- [19] Al-Tikrity, E.T., Yaseen, A.A., Yousif, E., Ahmed, D.S., I-Mashhadani, M.H. (2022). Impact on poly (Vinyl chloride) of trimethoprim schiff bases as stabilizers. *Polymers and Polymer Composites*, 30: 1-11. <https://doi.org/10.1177/09673911221094020>
- [20] Naoom, N., Yousif, E., Ahmed, D.S., Kariuki, B.M., El-Hiti, G.A. (2022). Synthesis of methyl dopa-in complexes and their applicability as photostabilizers for the protection of polyvinyl chloride against photolysis. *Polymers*, 14(21): 4590. <https://doi.org/10.3390/polym14214590>
- [21] Huang, R., Meng, J., Jiang, X. (2026). Degradation and utilization of polyvinyl chloride (PVC): Challenges and opportunities toward a circular economy. *Green Energy & Environment*, 11(2): 283-16. <https://doi.org/10.1016/j.gee.2025.10.010>
- [22] Ali, W.B., Salman, S.M., Farhan, M.A., Hassan, E.A. (2025). Synthesis and biological evaluation of new dihydrobenzo[e]indole-based schiff derivatives with straight and branched alkyl substituents. *International Journal of Design & Nature and Ecodynamics*, 20(7): 1565-1572. <https://doi.org/10.18280/ij dne.200713>
- [23] Saleh, T.A., Al-Tikrity, E.T.B., Ahmed, D.S., El-Hiti, G.A., Kariuki, B.M., Yaseen, A.A., Ahmed, A., Yousif, E. (2022). Monitoring physicochemical properties of transparent PVC films containing captopril and metal oxide nanoparticles to assess UV blocking. *Journal of Polymer Research*, 29(6): 249. <https://orca.cardiff.ac.uk/id/eprint/151514>
- [24] Nief, O.A. (2017). Synthesis and identification of heterocyclic compounds (oxazepine, tetrazole) derived from benzidine as photostabilizing for poly vinyl chloride. *Al-Mustansiriyah Journal of Science*, 28(2): 108-118. <https://doi.org/10.23851/mjs.v28i2.521>
- [25] Ziegenbalg, D., Wriedt, B., Kreisel, G., Kralisch, D. (2016). Investigation of photon fluxes within microstructured photoreactors revealing great optimization potentials. *Chemical Engineering & Technology*, 39(1): 123-34. <https://doi.org/10.1002/ceat.201500498>
- [26] Kamil, A. (2018). Chemical modification of poly (vinyl chloride) resin to improve the photostability processes. *Al-Nahrain Journal of Science*, 21(4): 1-9. <https://doi.org/10.22401/ANJS.21.4.01>
- [27] Masuelli, M.A. (2014). Mark-Houwink parameters for aqueous-soluble polymers and biopolymers at various temperatures. *Journal of Polymer and Biopolymer Physics Chemistry*, 2(2): 37-43. <https://doi.org/10.12691/jpbpc-2-2-2>
- [28] Liu, J., Lv, Y., Luo, Z., Wang, H., Wei, Z. (2016). Molecular chain model construction, thermo-stability, and thermo-oxidative degradation mechanism of poly (vinyl chloride). *RSC Advances*, 6(38): 31898-31905. <https://doi.org/10.1039/C6RA02354A>
- [29] Sitorus, B., Malino, M.B. (2021). Electrical conductivity of conducting polymer composites based on conducting polymer/natural cellulose. *Elkha*, 13(1): 84-89. <https://doi.org/10.26418/elkha.v13i1.46048>
- [30] Mayder, D.M., Tonge, C.M., Nguyen, G.D., Tran, M.V., Tom, G., Darwish, G.H., Gupta, R., Lix, K., Kamal, S., Kamal, S. (2021). Polymer dots with enhanced photostability, quantum yield, and two-photon cross-section using structurally constrained deepblue fluorophores. *Journal of the American Chemical Society*, 143(41): 16976-6992. <https://doi.org/10.1021/jacs.1c06094>

- [32] Ibrahim, W.A., Farhan, M.A., Abdulateef, M.H. (2020). Synthesis and evaluation of biological activity of some newsalicylic acid derivatives. *Biochemical and Cellular Archives*, 20(9): 3727-3732. <https://connectjournals.com/pages/articledetails/toc032159>
- [33] Balakit, A.A., Ahmed, A., El-Hiti, G.A., Smith, K., Yousif, E (2015). Synthesis of new thiophene derivatives and their use as photostabilizers for rigid poly (vinyl chloride). *International Journal of Polymer Science*, 2015(1): 510390. <https://doi.org/10.1155/2015/510390>
- [34] Mohammed, R., El-Hiti, G.A., Ahmed, A., Yousif, E. (2017). Poly(vinyl chloride) doped by 2-(4-isobutylphenyl)propanoate metal complexes: Enhanced resistance to UV irradiation. *Arabian Journal for Science and Engineering*, 42: 4307-4315. <https://doi.org/10.1007/s13369-016-2323-z>
- [35] Farhan, M.A., Abd, L.S., Mahmoud, Z.H. (2026). Development and analysis of PVC glass slides for urine microstructure studies. *South African Journal of Chemical Engineering*, 55: 575-585. <https://doi.org/10.1016/j.sajce.2025.12.018>
- [36] Figueroa-Ariza, L., Paez-Sierra, B. (2026). Solvent-dependent spectral deconvolution of amino-substituted chalcones: UV-is and FT-IR analysis supported by TD-DFT calculations. *Journal of Molecular Structure*, 1351(1): 1-11. <https://doi.org/10.1016/j.molstruc.2025.144083>
- [37] Farhan, M.A., Ali, W.B., Ibrahim, W.A., Mahmoud, Z.H. (2024). Anti-cancer schiff bases as photostabilizer for poly(vinyl chloride). *Bulletin of the Chemical Society of Ethiopia*, 38(1): 135-146. <https://dx.doi.org/10.4314/bcse.v38i1.11>
- [38] Amiri, O., Salavati-Niasari, M., Mir, N., Beshkar, F., Saadat, M., Ansari, F. (2018). Plasmonic enhancement of dye-sensitized solar cells by using Au-decorated Ag dendrites as a morphology-engineered. *Renewable Energy*, 125: 590-598. <https://doi.org/10.1016/j.renene.2018.03.003>
- [39] Farha, M.A., Mahmoud, Z.H., Falih, M.S. (2018). Synthesis and characterization of TiO₂/Au nanocomposite using UV-Irradiation method and its photocatalytic activity to degradation of methylene blue. *Asian Journal of Chemistry*, 30(5): 1142-1146. <https://doi.org/10.14233/ajchem.2018.21256>
- [40] Yousif, E., Hasan, A. (2015). Photostabilization of poly(vinyl chloride)-still on the run. *Journal of Taibah University for Science*, 9(4): 421-448. <https://doi.org/10.1016/j.jtusci.2014.09.007>
- [41] Yousif, E., Al-Amiery, A.A., Kadhum, A., Kadhum, A.A.H., Mohamad, A.B. (2015). Photostabilizing efficiency of PVC in the presence of schiff bases as photostabilizers. *Molecules*, 20(11): 19886-19899. <https://doi.org/10.3390/molecules201119665>
- [42] El-Hiti, G.A., Ahmed, D.S., Yousif, E., Al-Khazrajy, O.S.A., Abdallah, M., Alanazi, S.A. (2021). Modifications of polymers through the addition of ultraviolet absorbers to reduce the aging effect of accelerated and natural irradiation. *Polymers*, 14(1): 20. <https://doi.org/10.3390/polym14010020>
- [43] Yousif, E., Bakir, E., Salimon, J., Salih, N. (2012). Evaluation of Schiff bases of 2, 5-dimercapto-1, 3, 4-thiadiazole as photostabilizer for poly (methyl methacrylate). *Journal of Saudi Chemical Society*, 16(3): 279-285. <https://doi.org/10.1016/j.jscs.2011.01.009>
- [44] Yousif, E., Haddad, R. (2013). Photodegradation and photostabilization of polymers, especially polystyrene. *SpringerPlus*, 2(1): 398. <https://doi.org/10.1186/2193-1801-2-398>
- [45] Yousif, E., Hasan, A., El-Hiti, G.A. (2016). Spectroscopic, physical and topography of photochemical process of PVC films in the presence of Schiff base metal complexes. *Polymers*, 8(6): 204. <https://doi.org/10.3390/polym8060204>

NOMENCLATURE

CI	The carbonyl index
\overline{M}_v	Viscosity average molecular weight
Φ_{cs}	The quantum yield of chain scission
PVC	Polyvinyl chloride

Greek symbols

λ_{max}	Maximum absorption peak
-----------------	-------------------------